

Improvement of ECG based Personal Identification Performance in Different Bathtub Water Temperature by CNN

Jianbo Xu

Biomedical Information Engineering Laboratory
The University of Aizu
Aizu-wakamatsu, Fukushima, Japan
d8211103@u-aizu.ac.jp

Peng Cui

Biomedical Information Engineering Laboratory
The University of Aizu
Aizu-wakamatsu, Fukushima, Japan
d8211107@u-aizu.ac.jp

Tianhui Li

Biomedical Information Engineering Laboratory
The University of Aizu
Aizu-wakamatsu, Fukushima, Japan
d8211109@u-aizu.ac.jp

Wenxi Chen

Biomedical Information Engineering Laboratory
The University of Aizu
Aizu-wakamatsu, Fukushima, Japan
wenxi@u-aizu.ac.jp

Abstract—This paper aims at exploring the variety of Electrocardiogram(ECG) interval and amplitude during different bathtub water temperature and eliminating their influence on personal identification with ECG. There are 10 subjects in the experiment, each subject collects 2 ECG recordings, each recording is at least 220 s. One recording is collected at 38 ± 0.5 °C bathtub water temperature and the other recording is collected at 42 ± 0.5 °C bathtub water temperature. All the raw ECG are removed baseline drift and normalized, then the R peaks are detected and all the R-R interval(RRI) and amplitude are calculated. Through statistical analysis method, we find that the median of RRI in low bathtub water temperature is bigger than in high bathtub water temperature for all subjects, and compared with low bathtub water temperature, the variety of R peaks amplitude has 3 situations in high bathtub water temperature: increase, decrease and unchanged. Then all the QRS complex are segmented and are taken as training data and test data. During the training stage, there are 3340 training datasets, 1670 training datasets are from low bathing water temperature and the other 1670 training datasets are from high bathing water temperature. In the testing stage, first we use 410 testing data which are from low bathtub water temperature to test the trained model, the best and robust identification rate is 87.07%, when we use the other 410 testing data which are from high bathtub water temperature to test the trained model, the best and robust identification rate is 87.32%. To the best of our knowledge, this is the first time to explore the variety of ECG interval and amplitude during different bathing water temperature. However, further improvements are still needed during different bathing environment.

Index Terms—ECG, interval, amplitude, influence, identification

I. INTRODUCTION

Hot spring and bathing are very popular in Japan. However, due to the increasing aging population, there are more and

This study was supported in part by the Competitive Research Fund 2019-P-21 of the University of Aizu.

more drowning accidents these years among some old people with heart diseases. The heart rate and ECG vary greatly before and after one person entering the bathtub, the main reason is the stimulation which is caused by hot water. If we can monitor the dynamic changes of heart rate and ECG in real-time during bathing and predict the health status, it will be helpful to reduce the drowning accidents. However, firstly we should know who is in the bathtub during bathing, so how to perform personal identification with ECG during bathing is the primary work we should do.

ECG is the electrical activity of the heart, the normal ECG waveform includes 3 main components: P wave, QRS complex and T wave, the details are shown in Fig. 1. P wave represents the depolarization of the atria, QRS complex represents the depolarization of the ventricles and T wave represents the repolarization of the ventricles[1]. Traditional measurement methods are usually placing several electrodes on the skin, it is noninvasive and convenient, which has become a standard tool in the daily clinical diagnosis for some cardiac diseases.

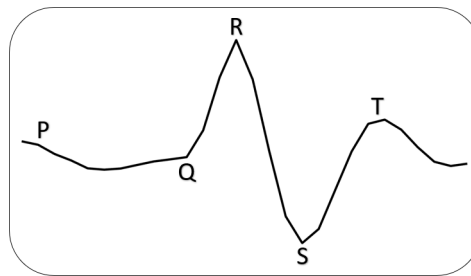


Fig. 1. Main components of the normal ECG waveform.

Because it exists in all the living creatures and has its unique characteristics, since L. Biel et al. investigated a new

approach for human identification with ECG during rest in 1999 [2], then more and more research in recent years regards ECG as a new biomedical personal identification tool [3–17]. Many previous published papers explored how to perform identification with ECG and achieved good results, however, only a few papers used bathtub ECG, and almost none papers explored the variety of ECG interval and amplitude during different bathtub water temperature.

In our previous study, we found that different bathtub water temperature had an important impact on personal identification. This paper aims at exploring the variety of ECG interval and amplitude during different bathtub water temperature and eliminating their influence on personal identification with ECG, and finally performing personal identification with ECG quickly and accurately in different bathtub water temperature. The final personal identification rates are 87.07% in low bathtub water temperature and 87.32% in high bathtub water temperature using the QRS complex of the ECG signal during bathing.

The rest of this paper is organized as follows: Section II gives the methods and materials, section III presents the results, and discussion and conclusion are proposed in Section IV and Section V respectively.

II. METHODS AND MATERIALS

A. Data collection system

The data collection system is shown in Fig. 2. There are 4 non-contact electrodes in the bathtub, which are placed near the right foot, right arm, left foot and left arm respectively, where one of the non-contact electrodes near right foot connects to ground. Lead I is the potential difference between the left arm and right arm, lead II is the potential difference between the left foot and right arm, and lead III is the potential difference between the left arm and left foot. The electricity arrives in the non-contact electrodes through the water, the non-contact electrodes and ECG amplifier are connected by a line, ECG amplifier is used to amplify the tiny potential difference until it can be recorded and observed. The ECG amplifier and computer are connected by Wi-Fi, all the collected data are stored in the computer ultimately.

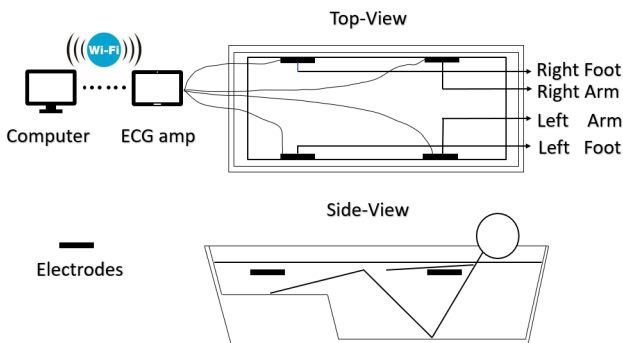


Fig. 2. Data collection system.

B. Subjects and ECG collection

There are 10 subjects in our experiment, including 5 males and 5 females, aged between 20 to 25 years old, the sampling rate of the data collection system is 100 Hz. During the data collection stage, first, we control the bathtub water temperature at 38 ± 0.5 °C and record the ECG. After 220 s, we increase the bathtub water temperature to 42 ± 0.5 °C and continue to record the ECG until the length of recording is more than 220 s.

C. Data processing and analysis

The collected data are segmented into 2 parts: 38 ± 0.5 °C recording and 42 ± 0.5 °C recording. For every recording, we use 220s data which belong to Lead II to do analysis.

In order to remove the baseline drift (low-frequency component), we use the 'db6' wavelet at level 4 to decompose the signal, then we reconstruct the signal using the function of 'waverec' after we subtract baseline drift (the final approximation coefficients) from the original signal and offset removed baseline, one of the output is shown in Fig. 3.

Then we normalized the preprocessed data into the range of 0 to 1 using the 'mapminmax' function, the equation is shown in (1):

$$y = \frac{x - x_{min}}{x_{max} - x_{min}} \quad (1)$$

where x is the input data, y is the output data, x_{max} is the maximal value of the input signal row vector, x_{min} is the minimal value of the input signal row vector.

Next, all the R peaks are detected by the function of 'findpeaks', where the 'MinPeakProminence' is 0.42. Then all the RRI and amplitude of R peaks are calculated, the details are shown in Fig. 4 and Fig. 5, where A to J represents every subject respectively, L represents 38 ± 0.5 °C bathtub water temperature and H represents 42 ± 0.5 °C bathtub water temperature.

Figure 4 shows that the median of RRI in low bathtub water temperature is bigger than in high bathtub water temperature for every subject. Figure 5 shows that compared with low bathtub water temperature, the variety of R peaks amplitude has 3 situations in high bathtub water temperature: the median of R peaks amplitude is obviously increasing for subject A, F, G, and J, and the median of R peaks amplitude is almost unchanged for subject B, D and H, however, the median of R peaks amplitude is obviously decreasing for subject C, E and I.

D. Data structure and CNN model design

Centering on the detected R peaks, we take 13 sampling points forward and 14 sampling points backward, we can segment the QRS complex, it is a 1×28 one-dimensional array.

For every subject, we select 235 QRS imaging respectively in each bathtub water temperature, taking 1st to 28th QRS as the first dataset and 2nd to 29th QRS as the second dataset, then we can get 208 datasets, selecting 167 (about 80%)

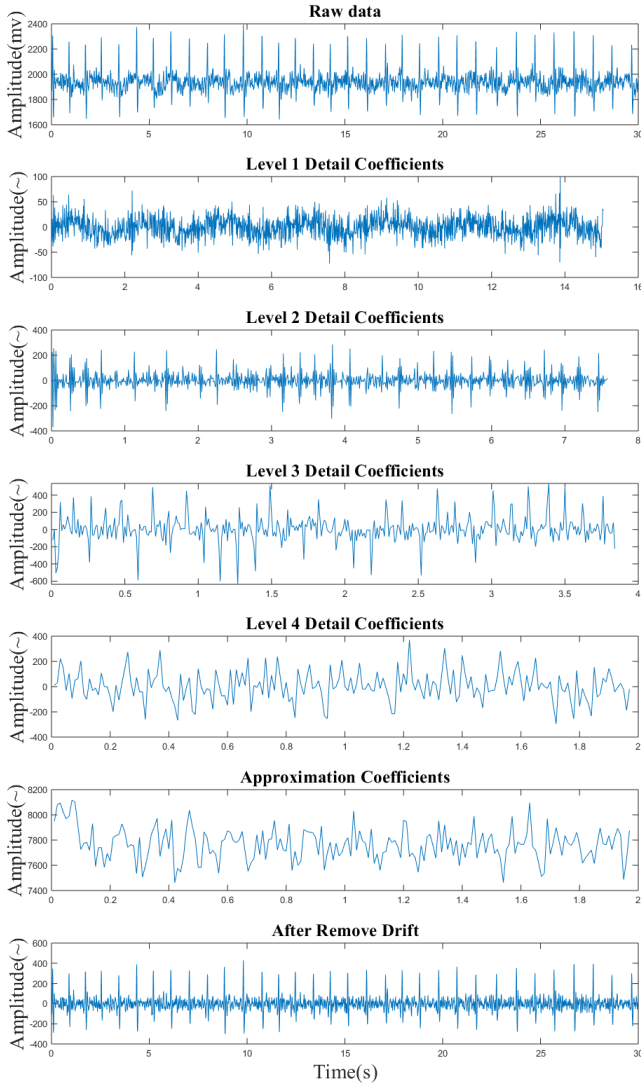


Fig. 3. Process of the ECG decomposition and reconstruction.

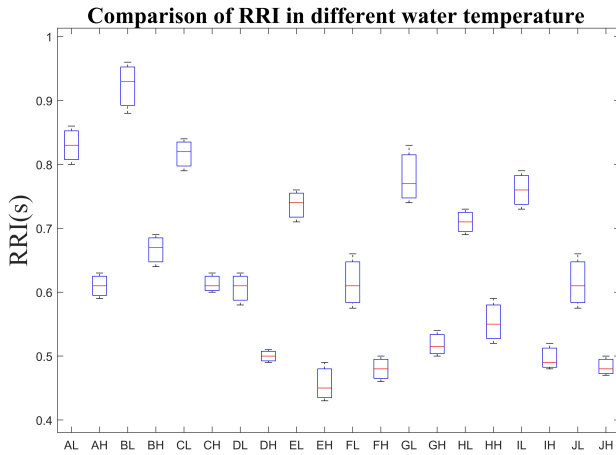


Fig. 4. Comparison of RRI in different bathtub water temperature.

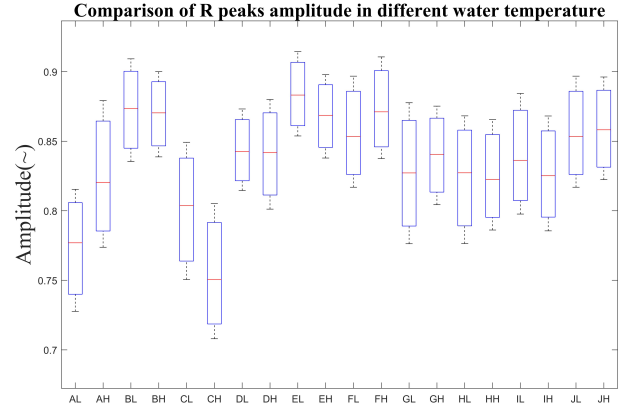


Fig. 5. Comparison of R peaks amplitude in different bathtub water temperature.

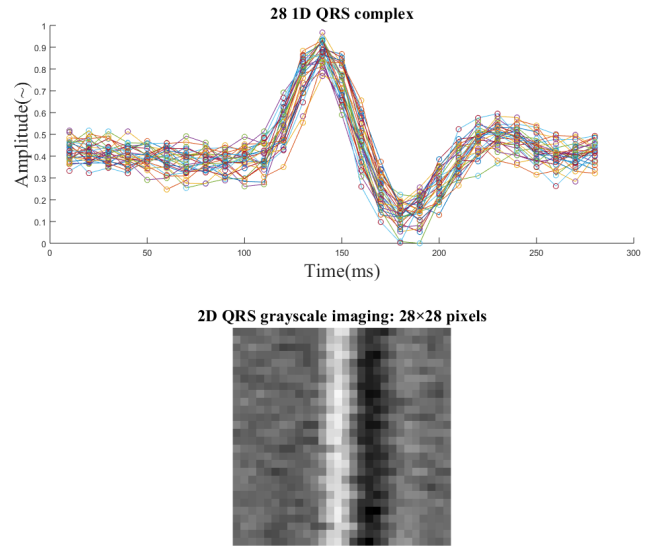


Fig. 6. 28 1D QRS complex to 2D QRS imaging.

datasets as the training data and 41 datasets (about 20%) as the testing data, one of the datasets is shown in Fig. 6.

Then, all the training data and testing data are put together respectively. At last, the size of `data_training_L` and `data_training_H` are $28 \times 28 \times 1670$ 3D array, the size of `data_testing_L` and `data_testing_H` are $28 \times 28 \times 410$ 3D array. We use 1 to 10 to mark every subject respectively, both of the `Labels_training_L` and `Labels_training_H` are a 1670×1 2D array, and the `Labels_testing_L` and `Labels_testing_H` are a 410×1 2D array.

There are 5 layers in the designed CNN model, the details are shown in Fig. 7.

In the input layer, the input data is a 28×28 grayscale. In the convolution layer, after performing convolution operation with 20 3×3 filters, the subsampling result is a $26 \times 26 \times 20$ 3D array. In pooling layer, the downsampling result is a $13 \times 13 \times 20$ 3D array. In the hidden layer, using fully connected

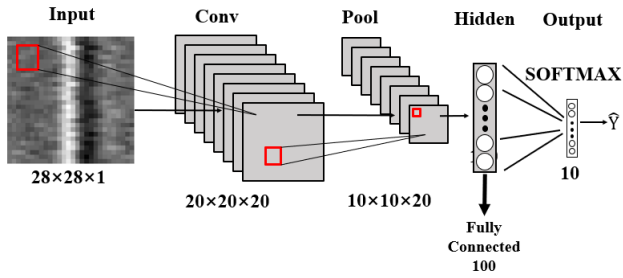


Fig. 7. CNN model.

method. In the output layer, using 'softmax' function to calculate the identification rate. There are 10 values in the output of 'softmax' function, every value indicates the possibility of every subject. If the row of the maximum of these 10 values in the 'softmax' function is same with the label of the input data, then let the accuracy increased by 1.

III. RESULTS

During the training process, before we performing data training, we firstly put the data_training_L and data_training_H together, and also put the Labels_training_L and Labels_training_H together, then we can get Data_training_all and Labels_training_all, and rearranging the order of Data_training_all and Labels_training_all.

During the testing process, first, we use data_testing_L to test the trained CNN model, the best and robust identification rate is 87.07%, and when we use data_testing_H to test the trained CNN model, the best and robust identification rate is 87.32%, the varieties of accuracy in the above 2 test processes are shown in Fig. 8.

IV. DISCUSSION

In our previous experiment, when we use the data which is collected in low bathtub water temperature ($38\pm 0.5\text{ }^{\circ}\text{C}$) to train and test the CNN model, the best and robust identification rate is 82.67%. However, if we use the data which is collected at high bathtub water temperature ($42\pm 0.5\text{ }^{\circ}\text{C}$) to test this trained CNN model directly, the identification rate is only 13.33%.

Similarly, if we use the data which is collected in high bathtub water temperature ($42\pm 0.5\text{ }^{\circ}\text{C}$) to train and test the CNN model, the best and robust identification rate is 85.50%. However, if we use the data which is collected at low bathtub water temperature ($38\pm 0.5\text{ }^{\circ}\text{C}$) to test this trained CNN model directly, the identification rate is only 12.17%.

In this paper, we explore the variety of RRI and amplitude of ECG during different bathtub water temperature using statistical analysis and find that the variation trend of RRI is definite, that is the median of RRI declines with the bathtub water temperature increasing. However, the variety of R peaks amplitude is uncertain in different bathtub water temperature: with the bathtub water temperature increasing, the median of R peaks amplitude is obviously increasing for subject A, F, G, and J, and the median of R peaks amplitude is almost

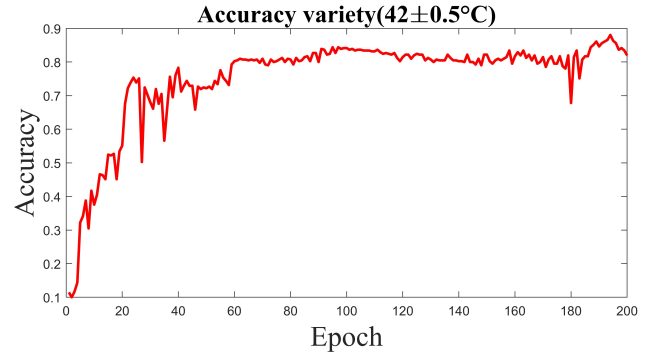
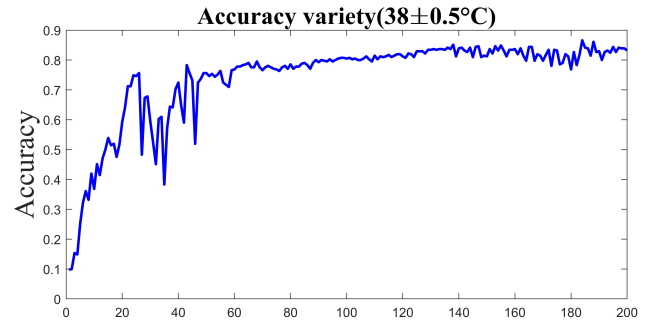


Fig. 8. Varieties of accuracy in testing process.

unchanged for subject B, D, and H, however, the median of R peaks amplitude is obviously decreasing for subject C, E and I. These varieties of RRI and amplitude further confirm the credibility of the experimental result in our previous paper.

In order to eliminate the influence of bathtub water temperature on personal identification with ECG, in this paper, the training data includes 2 parts, one half is collected in low bathtub water temperature ($38\pm 0.5\text{ }^{\circ}\text{C}$) and the other half is collected in high bathtub water temperature ($42\pm 0.5\text{ }^{\circ}\text{C}$). In the final testing stage, first, we use data_testing_L to test the trained CNN model, the best and robust identification rate is 87.07%, and when we use data_testing_H to test the trained CNN model, the best and robust identification rate is 87.32%.

V. CONCLUSION

In this paper, we explore the RRI and amplitude of ECG during different bathtub water temperature using statistical analysis method, the median varieties of RRI and amplitude preliminarily interpret the reason of the impact of bathtub water temperature on personal identification with bathtub ECG. The experimental results in this paper suggest that the designed CNN model can successfully perform personal identification with ECG at least in 2 different bathtub water temperature.

ACKNOWLEDGMENT

The authors thank all participants for their cooperation in data collection.

REFERENCES

- [1] Leonard S Lilly. *Pathophysiology of heart disease: a collaborative project of medical students and faculty*. Lippincott Williams & Wilkins, 2012.
- [2] Lena Biel, Ola Pettersson, Lennart Philipson, and Peter Wide. Ecg analysis: a new approach in human identification. In *IMTC/99. Proceedings of the 16th IEEE Instrumentation and Measurement Technology Conference (Cat. No. 99CH36309)*, volume 1, pages 557–561. IEEE, 1999.
- [3] S Zahra Fatemian and Dimitrios Hatzinakos. A new ecg feature extractor for biometric recognition. In *2009 16th international conference on digital signal processing*, pages 1–6. IEEE, 2009.
- [4] Chuang-Chien Chiu, Chou-Min Chuang, and Chih-Yu Hsu. A novel personal identity verification approach using a discrete wavelet transform of the ecg signal. In *2008 International Conference on Multimedia and Ubiquitous Engineering (mue 2008)*, pages 201–206. IEEE, 2008.
- [5] Tilendra Choudhary and M Sabarimalai Manikandan. A novel unified framework for noise-robust ecg-based biometric authentication. In *2015 2nd International Conference on Signal Processing and Integrated Networks (SPIN)*, pages 186–191. IEEE, 2015.
- [6] Hyun-Soo Choi, Byunghan Lee, and Sungroh Yoon. Biometric authentication using noisy electrocardiograms acquired by mobile sensors. *IEEE Access*, 4:1266–1273, 2016.
- [7] Fabienne Porée, Antoine Gallix, and Guy Carrault. Biometric identification of individuals based on the ecg. which conditions? In *2011 Computing in Cardiology*, pages 761–764. IEEE, 2011.
- [8] Youssef Gahi, Meryem Lamrani, Abdelhak Zoglat, Mouhcine Guennoun, Bill Kapralos, and Khalil El-Khatib. Biometric identification system based on electrocardiogram data. In *2008 New Technologies, Mobility and Security*, pages 1–5. IEEE, 2008.
- [9] Wael Louis, Majid Komeili, and Dimitrios Hatzinakos. Continuous authentication using one-dimensional multi-resolution local binary patterns (1dmrlbp) in ecg biometrics. *IEEE Transactions on Information Forensics and Security*, 11(12):2818–2832, 2016.
- [10] Min-Gu Kim and Sung Bum Pan. Deep learning based on 1-d ensemble networks using ecg for real-time user recognition. *IEEE Transactions on Industrial Informatics*, 2019.
- [11] Juan Sebastian Arteaga-Falconi, Hussein Al Osman, and Abdulmotaleb El Saddik. Ecg authentication for mobile devices. *IEEE Transactions on Instrumentation and Measurement*, 65(3):591–600, 2015.
- [12] Shin Jae Kang, Seung Yong Lee, Hyo Il Cho, and Hyunggon Park. Ecg authentication system design based on signal analysis in mobile and wearable devices. *IEEE Signal Processing Letters*, 23(6):805–808, 2016.
- [13] Chee-Ming Ting and Sh-Hussain Salleh. Ecg based personal identification using extended kalman filter. In *10th International Conference on Information Science, Signal Processing and their Applications (ISSPA 2010)*, pages 774–777. IEEE, 2010.
- [14] Foteini Agrafioti and Dimitrios Hatzinakos. Ecg based recognition using second order statistics. In *6th Annual Communication Networks and Services Research Conference (cnsr 2008)*, pages 82–87. IEEE, 2008.
- [15] Stanislaw Osowski and Tran Hoai Linh. Ecg beat recognition using fuzzy hybrid neural network. *IEEE Transactions on Biomedical Engineering*, 48(11):1265–1271, 2001.
- [16] Konstantinos N Plataniotis, Dimitrios Hatzinakos, and Jimmy KM Lee. Ecg biometric recognition without fiducial detection. In *2006 Biometrics symposium: Special session on research at the biometric consortium conference*, pages 1–6. IEEE, 2006.
- [17] Ikenna Odinaka, Po-Hsiang Lai, Alan D Kaplan, Joseph A O’Sullivan, Erik J Sirevaag, and John W Rohrbaugh. Ecg biometric recognition: A comparative analysis. *IEEE Transactions on Information Forensics and Security*, 7(6):1812–1824, 2012.